International Journal of Hydrogen Energy 90 (2024) 1012–1022

Contents lists available at ScienceDirect

International Journal of Hydrogen Energy

journal homepage: www.elsevier.com/locate/he

A critical evaluation of platinum deposition techniques for hydrogen production in microbial electrolysis cells

Pilar Sánchez-Peña [a], Jesús Rodriguez [b], Juan Antonio Baeza [a], David Gabriel [a], Albert Guisasola [a,*], Mireia Baeza [a,c]

[a] GENOCOV, Departament d'Enginyeria Química, Biològica i Ambiental, Escola d'Enginyeria, Universitat Autònoma de Barcelona, 08193, Bellaterra, Spain
[b] Centro Nacional Del Hidrógeno, 13500, Puertollano, Spain
[c] GENOCOV, Departament de Química, Facultat de Ciències, Edifici C-Nord, Universitat Autònoma de Barcelona, 08193, Bellaterra, Spain

ARTICLE INFO

Handling Editor: Jinlong Gong

Keywords:
Brush painting
Doctor blade
Electrospray
Microbial electrolysis cell
Spray
Sputtering

ABSTRACT

Despite its high cost, Pt is the usual catalyst for hydrogen production in the cathode of Microbial Electrolysis Cells (MECs). Its effectiveness depends not only on the amount deposited but also on the availability and distribution of Pt nanoparticles on the cathode surface. This work provides a comprehensive study of the effectiveness of the Pt coating with five deposition techniques: spray, electrospray, brush painting, doctor blade and sputtering. The performance of the cathodes was studied with different Pt loadings by monitoring the current intensity and H_2 production in MECs. Furthermore, cathodes were characterized morphologically using scanning electron microscopy together with energy-dispersive X-ray spectroscopy to study their Pt surface distribution and composition. Sputtering was initially discarded due to Pt detachment. When using the same amount of Pt (0.50 mg Pt cm^{-2}), the highest current density was obtained for electrospray (2.0 mA cm^{-2}), followed by spray (1.9 mA cm^{-2}), brush painting (1.6 mA cm^{-2}) and doctor blade (1.2 mA cm^{-2}). Hence, electrospray improved 20 % the results obtained by the default method of brush painting. Electrospray and spray provided better performance because of the direct deposition of Pt on the carbon fibres creating a compact Pt layer on the electrode surface. Furthermore, it was observed that the cell performance decreased significantly with decreasing amount of Pt per cm^2, observing the best performance with the highest Pt load tested (0.5 mg Pt cm^{-2}) regardless of the deposition technique.

1. Introduction

Due to the growing global economy and industrialization, the world energy demand has increased considerably in the last decade. Currently, the main energy source (>86 %) is derived from fossil fuels (oil, coal, and natural gas) which are finite and result in high CO_2 emissions [1]. In this context, renewable energies, such as solar, wind, and hydraulic among others are being promoted. Hydrogen (H_2) emerges as a promising energy vector because: (i) is a clean and renewable energy [2], (ii) does not contribute to CO_2 emissions [3], (iii) has a high specific heat of combustion (142.9 kJ g^{-1}) compared to other fuels (methane, 55.7 kJ g^{-1} or ethanol 29.7 kJ g^{-1}) [4], (v) is abundant as an elementary atom [3] and (vi) is easy to convert to other forms of energy as raw material [5].

Nowadays, the most sustainable approach for producing H_2 is the well-known concept of Power-to-gas (P2G), *i.e.* integration of water electrolysis and renewable energies to produce a gaseous fuel. However, water electrolysis requires high purity water, which is estimated to account for 12 % of CAPEX [6]. Wastewater as a feedstock for H_2 production is a promising alternative that allows to simultaneously exploit the energy potential of wastewaters [7,8] while avoiding an energy-intensive treatment such as activated sludge. However, the low conductivity, high complexity of wastewaters and the potential presence of harmful compounds for the catalysts have prevented water electrolysis technologies to grow in this field [9].

Bioelectrochemical techniques and, particularly, Microbial Electrolysis Cells (MECs) are a novel and promising approach for H_2 production from organic matter, including wastewater and other renewable resources that fit in the recent paradigm shift of circular economy [10,11]. An MEC is a bioelectrochemical system (BES) with a microbially colonised anode and a cathode [12]. Organic matter is oxidized by electroactive bacteria able to extracellularly transfer the electrons to the anode while generating CO_2 and protons (eq. (1)). Electrons travel to the

* Corresponding author.
E-mail address: albert.guisasola@uab.cat (A. Guisasola).

https://doi.org/10.1016/j.ijhydene.2024.09.341
Received 15 July 2024; Received in revised form 20 September 2024; Accepted 24 September 2024
Available online 10 October 2024

cathode through the external circuit and reduce either protons or water to H_2 (eq. (2) and eq. (3)) [13].

$$CH_3COO^- + 2H_2O \rightarrow 2\ CO_2 + 7\ H^+ + 8\ e^- \quad \text{(eq. 1)}$$

$$8\ H^+ + 8\ e^- \rightarrow 4H_2 \quad \text{(eq. 2)}$$

$$4H_2O + 8\ e^- \rightarrow 4H_2 + 8\ OH^- \quad \text{(eq. 3)}$$

If acetate is the electron donor, the electromotive force is −0.13 V under standard biological conditions (T = 25 °C and pH = 7), leading to a positive Gibbs energy (93.14 kJ mol^{-1}) [14]. Therefore, the MEC requires an externally supplied voltage (typically between 0.6 and 1.0 V depending on the specific overpotential) for H_2 production at the cathode [15,16]. Furthermore, this reaction has slow kinetics and it is heavily dependent on the catalyst deposited on the cathode electrode [17]. The most common catalyst used is platinum (Pt) because of its superior performance [18,19]. However, alternatives are currently sought because of its elevated market price [20–22]. The most widespread technique for the fabrication of Pt-coated cathodes in BES is brush painting, which consists of using a brush to deposit a catalyst ink on the carbon support surface [23]. Being a handmade technology, cathode production costs are reasonable at expenses of poor precision and reproducibility. Thus, brush painting results are particularly suitable for lab applications [23,25]. Nevertheless, the large amount of Pt used (0.5 mg Pt cm^{-2}) and the handmade approach discourages its use for full-scale applications. Novel techniques for Pt deposition are needed to optimize production costs by using the strictly necessary amount of Pt while improving BES operation. For instance, the overlapping of Pt atoms should be avoided because only the layer which is in contact with the mineral medium will catalyse hydrogen evolution reaction (HER). Moreover, these alternative methodologies should be easily scalable to bridge the current gap between lab-scale and full-scale MECs development.

In this regard, this work analyses five different Pt-deposition methodologies to obtain low, or even ultra-low, Pt-loaded electrodes with a scaling-up perspective: brush painting, doctor blade (tape-casting), spray, electrospray and sputtering. These techniques are widely used in the fabrication of proton exchange membranes (PEMs) for solid oxide electrochemical systems [26,27] and have scarcely been applied in MECs.

Doctor blade is broadly used for the fabrication of electrodes in different applications beyond fuel cells such as photoelectrochemistry [29] or organic solar cells [21]. Electrodes are produced by the deposition of a catalyst slurry on the support, which is then spread by a blade or similar. Doctor blade is more precise than hand-painting methods, however, its accuracy strongly depends on the slurry composition, its rheologic properties and the morphology of the support. Doctor blade has only been applied in smooth surfaces such as cation exchange membranes [30] or in photo-microbial fuel cells [31], while it has been barely used for the deposition of catalysts over carbon supports in BES. Li et al. [24] deposited sulphur polypyrrole onto carbon fibre paper (CFP) using doctor blade as the first step of the fabrication of CoNi-based cathodes for MECs.

Spraying has been used for PEM fabrication since the eighties, and currently, it is used for the deposition of the catalyst layer in PEM-based fuel cells at industrial scale. Different approaches have been applied such as spraying of a Pt ink on the carbon support [32] or directly over the membrane [33]. Although alternative methodologies have been proposed [34,35], the catalyst ink should be homogenized employing a spraying process [36]. Once the ink is homogenized, it is sprayed over a support by using an airbrush (manually or automated) while promoting the evaporation of the solvent, for example using a hot plate or using an IR lamp. In MECs, spraying has gained attention for the fabrication of low-cost cathodes by deposition of different Pt-free catalysts. Manuel et al. [28] prepared cathodes for H_2 production by spraying two types of catalytic inks on carbon paper: a multicomponent ink containing Ni, Mo, Cr, and Fe (total catalyst load of 1 mg cm^{-2}) and ink with only Ni (0.6 mg cm^{-2}). Ghasemi et al. [39] reported the fabrication of a new cathode based on spraying polyaniline and graphene on a stainless-steel mesh.

Electrospray (or electrospinning) is a recent and precise technique for nanoparticle synthesis or deposition [38]. It comprises the electro-atomization of a colloidal suspension of catalyst particles by the application of a high voltage difference between an ejector needle and the collecting support. Electrospray allows the fabrication of ultra-low Pt-loaded cathodes (as low as 0.012 mg Pt cm^{-2} [40]) with a uniform distribution of catalyst nanoparticles, resulting in highly efficient catalyst utilization [41,42]. Since the first reported application on PEM fuel cells in 2005 [41], the use of electrospray has been growing in the last decade but rarely in the BES field. Electrospray has only been applied for the fabrication of carbon nanofibers support for anodes [43] or membranes [44].

Sputtering provides dense catalyst layers with ultra-low Pt loadings [45], even lower than those in electrospray (down to 0.001 mg Pt cm^{-2}) [46]. Lefevre et al. [47] prepared ultra-low Co- and Pt-loaded cathodes (0.01 mg Pt cm^{-2}) for oxygen reduction in a microbial full cell (MFC) and compared its performance against a commercial 0.5 mg Pt cm^{-2} cathode. Interestingly, the Co-based cathode reported only less 27 % power than the commercial Pt cathode (with 5 times higher loading). Sputtering has rarely been used in MECs. To the best or our knowledge, sputtering was used for the simultaneous phosphorus recovery and H_2 production as Pt-sputtered carbon felt cathodes [37,48].

Each of the mentioned techniques exhibits promising potential for cathode optimization in BES. Nevertheless, it is crucial to understand their respective advantages and disadvantages before implementation. In this work, five different techniques, namely brush painting, spray, electrospray, sputtering, and doctor blade, are compared for the first time for Pt deposition on the cathode of the same experimental MEC configuration to minimise the Pt loading on the cathode, one of the main bottlenecks for its economic feasibility. Furthermore, cathodes with different Pt loadings (from 0.01 to 0.5 mg Pt cm^{-2}) were prepared to understand the effectiveness of the different coating methods even at low Pt loadings.

2. Materials and methods

2.1. Microbial electrolysis cell construction

The single-chamber MEC used in this work (Fig. 1a) consisted of a 35 mL cube cell of methacrylate (4.4 cm length x 5 cm width x 5 cm height) with a glass tube (7.7 cm height x 2 cm diameter) connected to a 100 mL gas bag to collect the produced gas (Fig. 1b) [49]. The main body was assembled with two lateral methacrylate endplates, using O-rings and gaskets to prevent electrolyte leakages. These pieces were kept together by tightening screw and wing nut [50].

The anode was a commercial graphite fibre brush (2.0 x 2.5 × 5.0 cm, Mill-rose, US) with a titanium wire as a current collector. This electrode was thermally treated in a muffle furnace at 450 °C for at least 30 min. This treatment allows both, the elimination of impurities and microfractures generation, leading to an increase in the active area and thus, enhancing biomass adhesion [51]. The cathode (7 cm^2) was based on treated carbon cloth. The catalyst used was Pt, coated with different techniques and Pt loads (mg Pt cm^{-2}). Pt-loads of 0.15, 0.3, and 0.5 mg Pt cm^{-2} were used for brush painting, doctor blade, spray and electrospray. Sputtering was investigated only with a Pt loading of 0.01 mg Pt cm^{-2} due to the long operation times of the deposition process. In all cases, cathodes were electrically connected to the carbon cloth support through a titanium wire.

2.2. Pt deposition procedures for cathode preparation

A schematic of the cathode preparation procedure by brush painting is shown in Fig. 2a. A paste or slurry with catalyst was obtained by

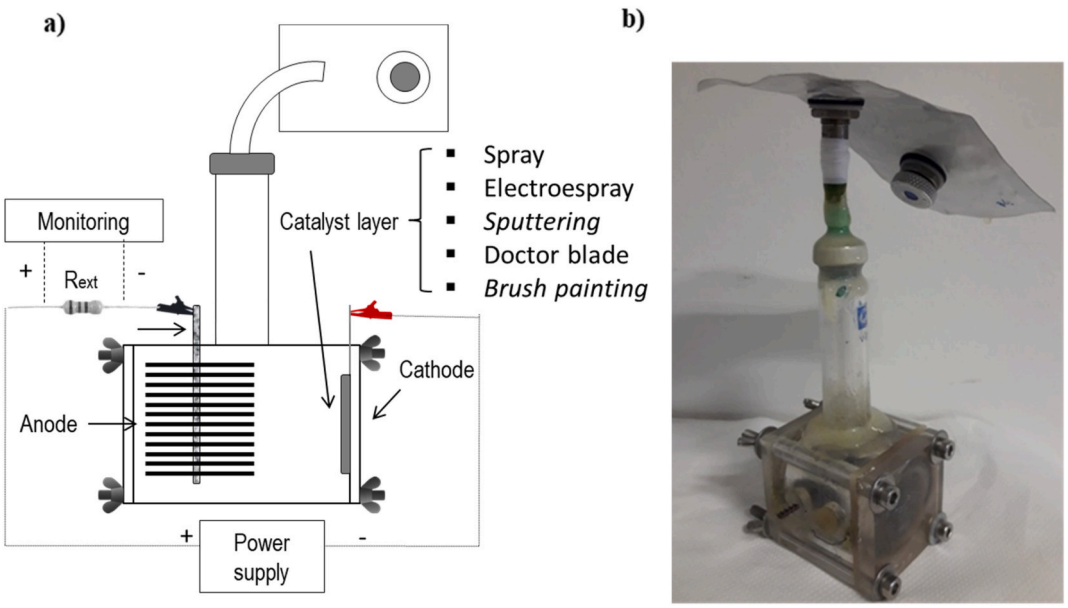

Fig. 1. Scheme (a) and picture (b) of a MEC used in this work.

mixing 10 % Pt/C (0.5 mg Pt cm^{-2}; Pt/C EC-10-PTC and 10 wt% Pt/VXC72 5 g) and Milli-Q water (4.15 μL cm^{-2}) for 20 s. Then, a mixture of Nafion (33.4 μL cm^{-2}, *Merck*) and 2-propanol (16.7 μL cm^{-2}, *Sigma Aldrich*) was added to obtain a binding paste which was stirred again. The resulting slurry was coated over the carbon cloth, using a thick brush. Finally, the coating was air-dried for 24 h.

In the case of doctor blade's method (Fig. 2b), the catalyst slurry for the cathodes was prepared following the same procedure as in the brush painting method. Then, the Pt slurry was coated over the carbon cloth, using a glass rod. After that, the coating was air-dried for 24 h, and a titanium wire was assembled to the cathode as an electrical connection. The same Pt load was used (0.5 mg Pt cm^{-2}) but with a homogeneous distribution of the catalyst slurry and a suitable viscosity which avoided the ink seepage through the carbon cloth.

The spraying procedure is depicted in Fig. 2c. The catalyst ink was prepared by mixing 20 % Pt/C (0.5 mg Pt cm^{-2}), Nafion 5 % (0.13 ± 0.02 mL cm^{-2}) and 2-propanol (between 4 and 8 mL cm^{-2}), and then homogenized using an ultrasound equipment during 2 h. Cathodes with different Pt-loads (0.13–0.24 mg Pt cm^{-2}) were obtained by using a hand-held VEGA 2000 airbrush [32]. Cathodes with 0.5 mg Pt cm^{-2}were prepared with a Nordson EFD Dispensing Robot with an integrated spray nozzle [42] because of the longer times required for the coating process. Cathodes were frequently weighed in a precision microbalance (CPA225D, Sartorius), with an accuracy of 0.1 mg to obtain the required coating load.

In the case of electrospray (Fig. 2d), the ink catalyst was prepared following the same procedure as in the spray technique. The resulting ink was coated over the carbon cloth support using a YFLow StartUp Lab Device (Yflow S.D., Spain) equipped with a flat collector (200 × 200 mm), using a simple injector with an external/internal diameter ratio of 0.9/0.6 mm [52]. The ink was introduced into 10 mL syringes and deposited at flow rates of 1 mL h^{-1}, an applied potential of 11–15 kV and 15–20 cm between the collector and the injector needle. Cathodes with different Pt-loads (0.15, 0.24 and 0.5 mg Pt cm^{-2}) were obtained by modifying the operation time, determined by weighing the electrodes.

A schematic of the sputtering procedure is depicted in Fig. 2e. The carbon substrate was coated by using a Leica EM ACE600 sputter coater (Leica Microsistemas S.L.U, Spain). Energetic argon-ions accelerated by a high voltage (3–5 kV) are forced to collide with a Pt plate and promote the extraction (sputtering) of Pt atoms, which are directed towards the carbon cloth, thereby forming a very thin film [53,54]. This technique resulted in the deposition of a thin layer (very few nanometres) of Pt. The cathodes had 20 nm of Pt, corresponding to 0.01 mg Pt cm^{-2}. Finally, the coating was air-dried for 24 h. The cathode was electrically connected by a titanium wire assembled to the carbon cloth support.

2.3. Experimental conditions

The anode was inoculated in an MFC, by mixing 14 mL of fresh medium and 14 mL of media from an already working inoculum-MFC [55]. The anode was assembled in an MEC once inoculated, *i.e.* when a stable current density was measured for several cycles. A voltage of 0.8 V was applied to each cell to drive the reactions.

The initial concentration of anhydrous sodium acetate (Ac^-) as the carbon source was about 1.5 g L^{-1}. The mineral medium composition for all cells contained (per L of Milli-Q-water) 15.09 g $Na_2HPO_4{\cdot}2H_2O$, 2.06 g KH_2PO_4, 0.2 g NH_4Cl, 4.0 mg $FeCl_2$, 6.0 mg Na_2S and 5 ml of nutrient solution, which contained per L: 1 g EDTA, 0.164 g $CoCl_2{\cdot}6H_2O$, 0.228 g $CaCl_2{\cdot}2H_2O$, 0.02 g H_3BO_3, 0.04 g $Na_2MoO_4{\cdot}2H_2O$, 0.002 g Na_2SeO_3, 0.02 g $Na_2WO_4{\cdot}2H_2O$, 0.04 g $NiCl_2{\cdot}6H_2O$, 2.32 g $MgCl_2$, 1.18 g $MgCl_2$, 1.18 g $MnCl_2{\cdot}4H_2O$, 0.1 g $ZnCl_2$, 0.02 g $CuSO_4{\cdot}5H_2O$, and 0.02 g $AlK(SO_4)_2$. All reagents were of analytical grade supplied by Scharlau SL (Spain). The initial pH and conductivity in the cells were around 7.5 and 13 mS cm^{-1}, respectively [56].

2.4. Analytical methods and instrumentation

Acetate was measured by gas chromatography (GC) (Agilent Technologies, 7820-A) using a flame ionization detector, DB-FFAB column, and helium as carrier gas. Samples for chemical analyses were taken at the beginning and the end of each cycle, accounting for a maximum of 10 % of the total reactor volume.

H_2, methane, and carbon dioxide were measured with a gas chromatograph equipped with two columns, a Porapaq Q 80/100 3 ft. G3591-81136 (1.38 m × 2 mm) packed column and a second column MolSieve 5A 80/100 3 ft. G3591-80017 (1.83 m × 2 mm) from Agilent Technologies. N_2 was used as carrier gas. The initial temperature of the oven was set at 70 °C for 2 min, followed by a temperature ramp of 20 °C· min^{-1} up to a temperature of 140 °C. Chromeleon 6.8 software (ThermoFisher Scientific) was used for data acquisition and signal processing.

Both electrodes were connected to a power supply (LABPS3005DN,

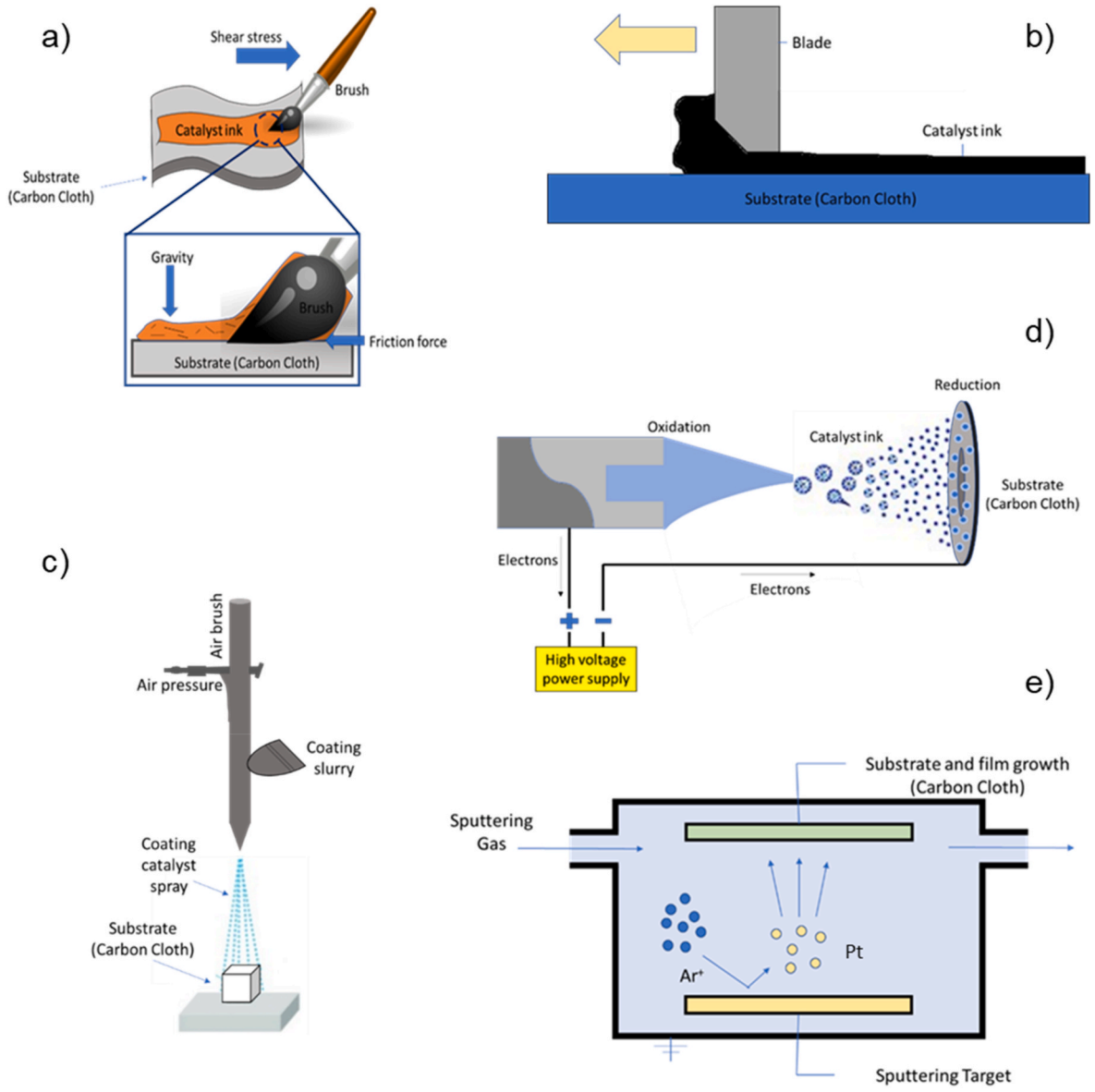

Fig. 2. Schematic of each deposition technique used: (a) brush painting, (b) doctor blade, (c) spray, (d) electrospray and (e) sputtering.

Velleman Group, Belgium) with 0.8 V as applied potential. The intensity was monitored by measuring the voltage evolution across a resistance (10 Ω) using a 16-bit data acquisition card (Advantech PCI-1716) connected to a personal computer with the Addcontrol software developed in LabWindows/CVI 2020 [56].

The morphology and composition of the cathode surface was assessed by Scanning Electron Microscopy (SEM) in a Merlin™ microscope (Carl Zeiss AG, Germany) and a Jeol JSM 6010 (JEOL Ltd, Tokyo, Japan) in *Centro Nacional del Hidrógeno* (Puertollano, Spain), both were equipped with an EDX analysis system [50].

2.5. MECs performance indices

The performance of the MECs was assessed through the calculation of the Coulombic Efficiency (CE), r_{CAT}, r_E, r_S, r_{E+S}, relative composition H_2, and H_2 production.

The CE (eq. (4)) compares the coulombs recovered as current intensity with the coulombs that could be theoretically generated from the substrate oxidation,

$$CE = \frac{\int_{t_0}^{t_F} I\,dt}{F \cdot b_S \cdot V_L \cdot \Delta C \cdot M_S^{-1}} \quad \text{(eq. 4)}$$

with t_0 and t_F (s) the initial and final time of the batch experiment, I (A) current, F (96485 C $mol^{-1} \cdot e^{-1}$) Faraday's constant, b_S (8 mol e^-/mol Ac^-) number of electrons transferred in the reaction per mole of the substrate, V_L (0.035 L) volume of the reactor, ΔC (g L^{-1}) substrate concentration change over a batch cycle and M_S (59 g mol^{-1}) molecular weight of the substrate.

MEC performance was also assessed by r_{CAT} (eq. (5)), which compares the coulombs consumed in H_2 production with the coulombs arriving at the cathode as current intensity,

$$r_{CAT} = \frac{b_{H_2} \cdot V_{H_2} \cdot F \cdot V_m^{-1}}{\int_{t_0}^{t_F} I\,dt} \quad \text{(eq. 5)}$$

with V_{H2} (L) volume of H_2 produced, b_{H2} number of moles of e^- transferred per mole of H_2 (2 mol e^- mol^{-1} H_2) and V_m (24.03 L mol^{-1}) molar gas volume at 20 °C and 1 atm [57].

The energy recovery of the cell, *i.e.* the amount of energy produced as

H_2 with respect to the energy supplied, was calculated with (i) the electrical input (r_E) (eq. (6)), (ii) the energy content of the substrate (r_S) (eq. (7)), and (iii) both the electrical input and the energy content of the substrate (r_{E+S}) (eq. (8)) as described [58],

$$r_E = \frac{W_{H_2}}{W_E} = \frac{n_{H_2} \cdot \Delta H_{H_2}}{\int_{t_0}^{t_F} (I \cdot E_{ap} - I^2 \cdot R_{ext})\,dt} \quad \text{(eq. 6)}$$

with W_{H2} (kJ) energy content of the produced H_2, W_E (kJ) energy input by the power supply, n_{H2} moles of produced H_2, ΔH_{H2} heat of combustion of H_2 (−285.83 kJ mol^{-1}) and E_{ap} (V) applied voltage,

$$r_S = \frac{W_{H_2}}{W_S} = \frac{n_{H_2} \cdot \Delta H_{H_2}}{n_S \cdot \Delta H_S} \quad \text{(eq. 7)}$$

with W_S (kJ) energy content of the substrate, n_S mols of consumed substrate and ΔH_S (kJ mol^{-1}) heat of combustion of the substrate (−870.28 kJ mol^{-1} for acetate).

$$r_{E+S} = \frac{W_{H_2}}{W_E + W_S} = \left(\frac{1}{r_E} + \frac{1}{r_S}\right)^{-1} \quad \text{(eq. 8)}$$

The H_2 relative composition in the cell was calculated as the ratio of H_2 to the total amount of H_2 and methane (eq. (9)),

$$\textit{Relative composition}_{H_2} = \frac{V_{H_2}}{V_{H_2} + V_{CH_4}} \quad \text{(eq. 9)}$$

with V_{H2} and V_{CH4} (L) volume obtained for H_2 and CH_4, respectively.

Gas composition was calculated according to the "Gas Bag Method" presented by Ambler and Logan [59]. The procedure followed consisted of first analysing the initial composition of the gas in the bag. Then, a known volume of tracer gas (carbon dioxide) was added to the gas bag using a gastight syringe (10 mL Hamilton Samplelock Syringe), and finally, the resulting mixture was again analysed. From these two analyses, mass balances were calculated, including the change in sample composition and the volume added, which allowed the calculation of the initial H_2 and methane volume (eq. (10)),

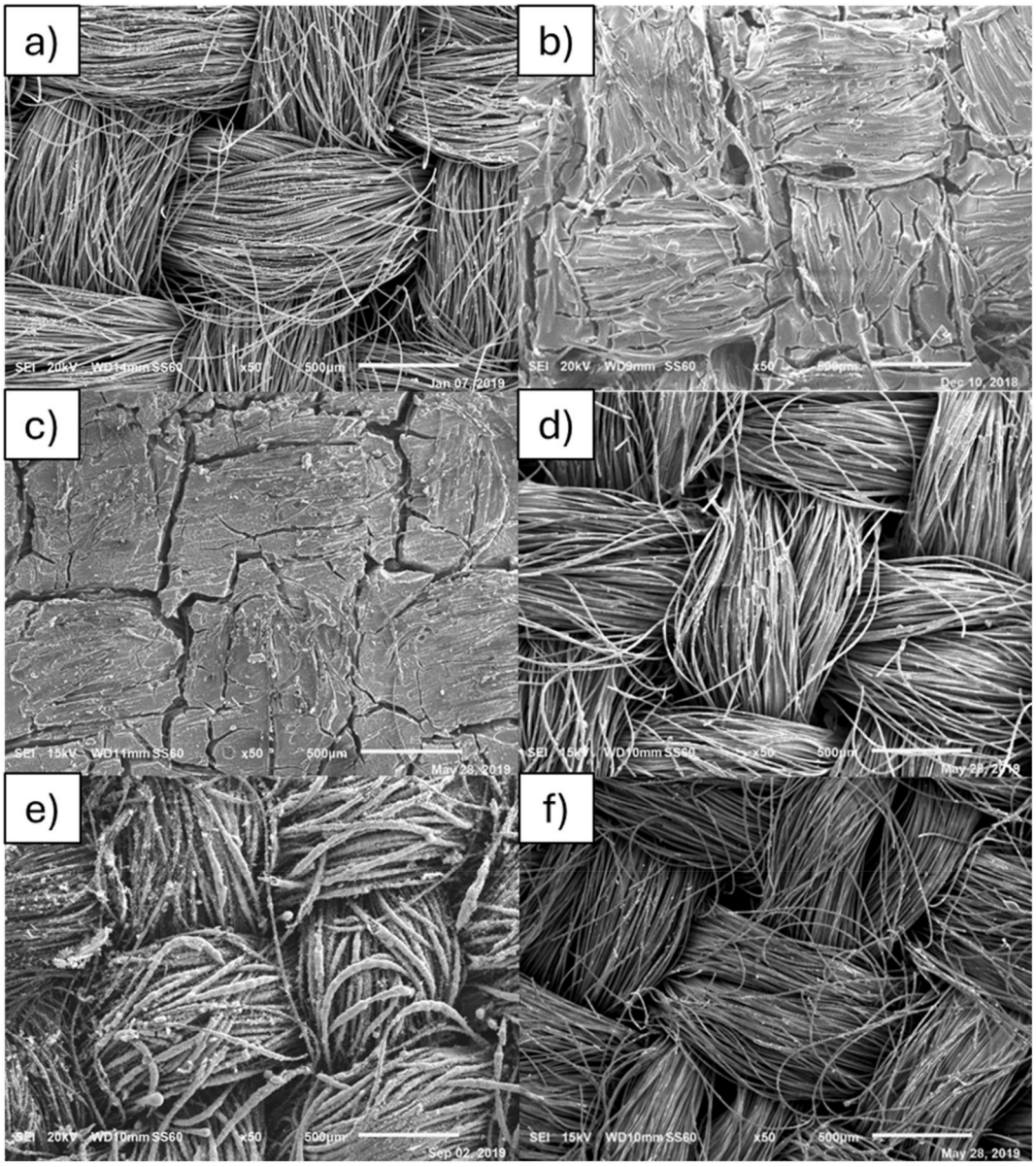

Fig. 3. SEM images obtained at ×50 magnification of (a) bare carbon cloth, (b) after brush painting, (c) after doctor blade, (d) after spraying, (e) after electrospraying and (f) after sputtering.

$$V_{total,initial} = \frac{V_{added,N_2}\left(1 - x_{run\ 2,N_2}\right) + V_{run\ 1}\left(x_{run\ 2,N_2} - x_{run\ 1,N_2}\right)}{x_{run\ 2,N_2} - x_{run\ 1,N_2}} \quad \text{(eq. 10)}$$

with $V_{total,\ initial}$ (L) initial total gas volume in the bag, $V_{added,\ N2}$ (L) known volume of nitrogen added, $V_{run\ 1}$ (L) volume injected in the GC in the first analysis, and x molar fraction of carbon dioxide in the first/second analysis as indicated on the subscript.

3. Results and discussion

3.1. Optical characterisation of the cathodes

The morphological characteristics of the cathodes fabricated with the five deposition techniques and their composition were studied through SEM. Fig. 3 shows the SEM images of the cathodes using the applied Pt deposition methodologies. All the cathodes in Fig. 3 contained 0.5 mg Pt cm^{-2} except for the sputtered one, which was only 0.01 mg Pt cm^{-2} as abovementioned. The SEM images for the electrodes manufactured by brush painting and doctor blade (Fig. 3b and c) showed a rigid and flat layer on the electrode surface where the individual fibres cannot be clearly distinguished. These cathodes exhibited cracks in the surface. In the case of doctor blade, the cracks were large and divided into square-shaped sections, apparently coinciding with the electrode material. More specifically, these cracks were associated with the warp and weft of the carbon cloth fibres used in the electrode construction. On the other hand, the brush-painted cathode showed numerous thin cracks distributed over the entire cathode surface. These cracks were due to the mechanical stress of the ink when becoming rigid after drying: that cracks led to an increase in the active area compared to an ink without cracks. In any case, the area was still lower than that obtained with techniques that do not generate a rigid layer, namely spray, electrospray, and sputtering (Fig. 3d, e and f). The sample prepared by doctor

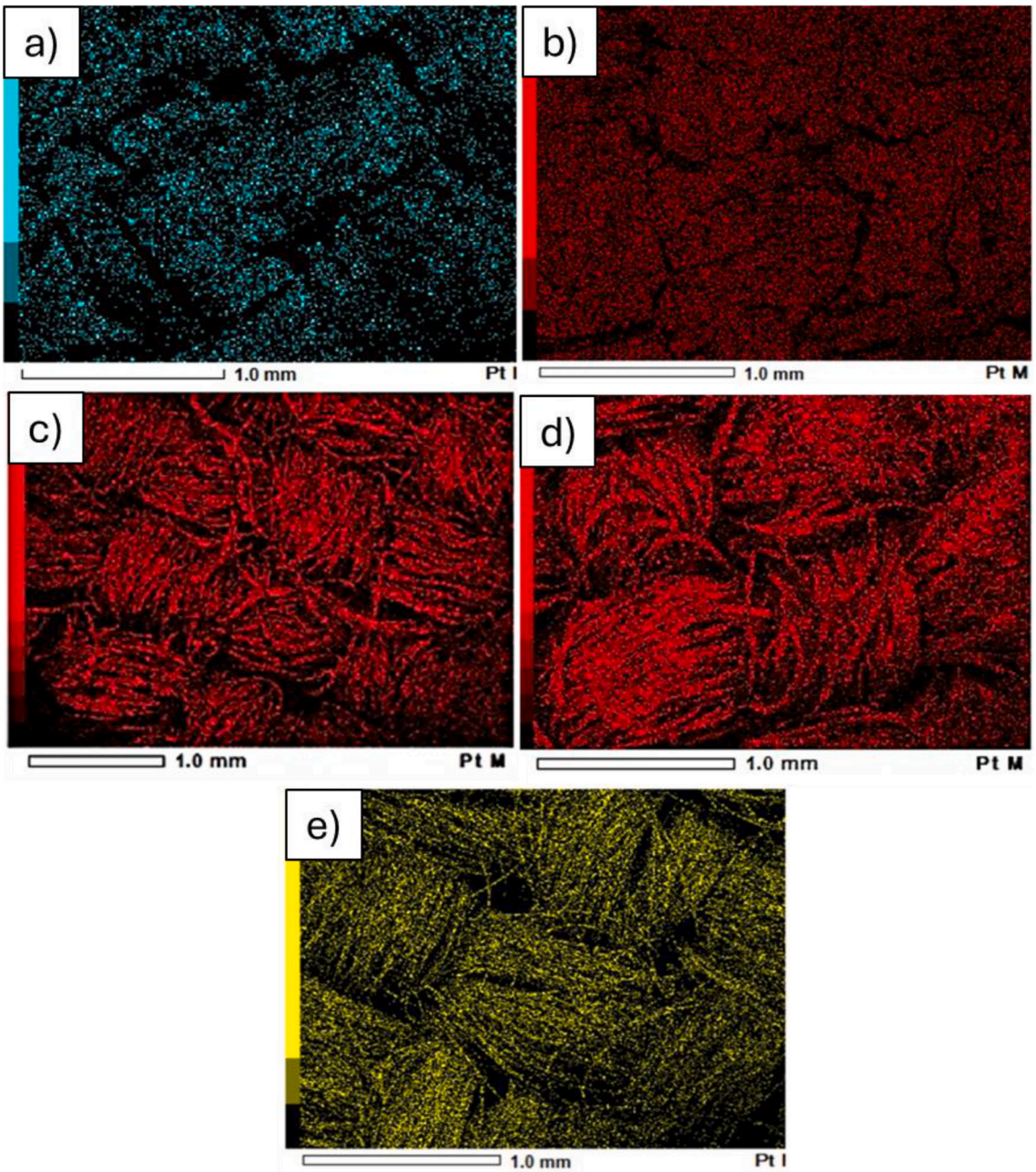

Fig. 4. EDX images of the Pt element for cathodes with (a) brush painting, (b) doctor blade, (c) sputtering, (d) electrospraying and (e) sputtering.

blade showed a smoother surface since the glass rod allows for a more even distribution. The brush painting technique is manual and, as such, brings high variability to the process and cannot guarantee a suitable control of the morphology and heterogeneity of the deposited layer.

Mapping of Pt with SEM-EDX images (Fig. 4) provided information about the catalyst distribution over the cathode. The SEM-EDX images of the cathodes show the Pt distribution on the electrode fibres. Although Pt is distributed over the entire surface, some differences can be identified: the Pt distribution looks like a compact ink with the brush painting and doctor blade technique (Fig. 4a and b) but, in the case of spray, electrospray and sputtering (Fig. 4c and d and e), the Pt is deposited more selectively on the electrode carbon fibres and Pt nanoparticles are observed on the surface.

Fig. 5 shows zoomed SEM images for spray, electrospray, and sputtering. The coating appears to be more effective on the outermost fibres (Fig. 5a and d). In fact, the most superficial fibres of the sprayed cathode are completely covered whereas only a partial coating is observed in the inner ones (Fig. 5a). Electrospray seems more effective on the outermost layers of carbon cloth, and internal fibres would only be covered under longer electrodeposition times, unfortunately resulting in higher ink requirements. The electrosprayed electrode displays a rougher coating in all its fibres (Fig. 5c). A similar morphology to the sprayed cathode was expected. Yet a continuous wrinkled ink layer was observed. Rugosity was expected to increase the electrode active area and catalyst accessibility, and thus, the cathodic performance. The difference between both spray and electrospray is that an electric field is applied in the latter. The sputtered cathode (Fig. 5d) shows a thinner, smooth, and uniform layer, due to the direct deposition of Pt atoms. Nevertheless, the covering range depends on the location of the fibres: the external ones showed a full coverage; intermediate fibres presented a partial Pt deposition, and deeper ones were practically uncoated.

The different morphologies of coatings are also related to the different properties of the catalyst ink (paste, slurry) required to drive the process. Doctor blade and brush painting needed high viscosity slurries, which generated an almost unique and continuous layer over the carbon fibres, which were hardly distinguished. Spraying techniques rely on the evaporation of the solvent. This allows particles to only deposit on the fibres, although, when spraying, a significant percentage of catalyst ink is lost due to the high porosity of the support. This loss was not observed in the case of the electrospray methodology since the electric field diverts the particles to the carbon fibres, allowing a thicker catalyst layer over the fibres and a more efficient and selective deposition (less catalyst ink losses) than spray. Finally, only Pt is used in the case of sputtering, with no application of an ink nor a slurry, thus selectively coating the conductive zones of the carbon support (*i.e.* the fibres).

From an economical point of view, minimizing the amount of Pt dosed is essential when using an expensive catalyst such as Pt. However, this Pt load reduction should not be at expenses of a much worse performance. All the Pt added must be accessible and exposed to the liquid to avoid a loss in the catalytic activity. Thus, a homogeneous distribution of a low amount of Pt nanoparticles is critical from both an economical and performance point of view. In this sense, spraying, electrospraying and sputtering methods seemed to be best candidates.

3.2. MEC performance for each cathode

The cathodes with different Pt deposition techniques and different Pt loadings were operated for long-term under batch conditions. Each cell operated for 115 days, performing a total of 23 cycles. Since each cell showed a similar behaviour along the operation, the current density of the first and last 15 days of operation of each cell with cathodes loaded with 0.5 mg Pt cm^{-2} (0.01 mg Pt cm^{-2} for the sputtered cathode) is shown in Fig. 6. Table 1 summarizes the performance of each cell with the different cathodes. The cathodes with Pt deposition using electrospray and spray showed the maximum current density among all techniques (2.0 and 1.9 mA cm^{-2}, respectively) and higher H_2 production rate (2.01 and 2.06 m^3 $m^{-3}d^{-1}$ of H_2, respectively). These methodologies showed a more accurate, selective, and efficient deposition. Brush painting showed at maximum of 1.6 mA cm^{-2} of current density, with a

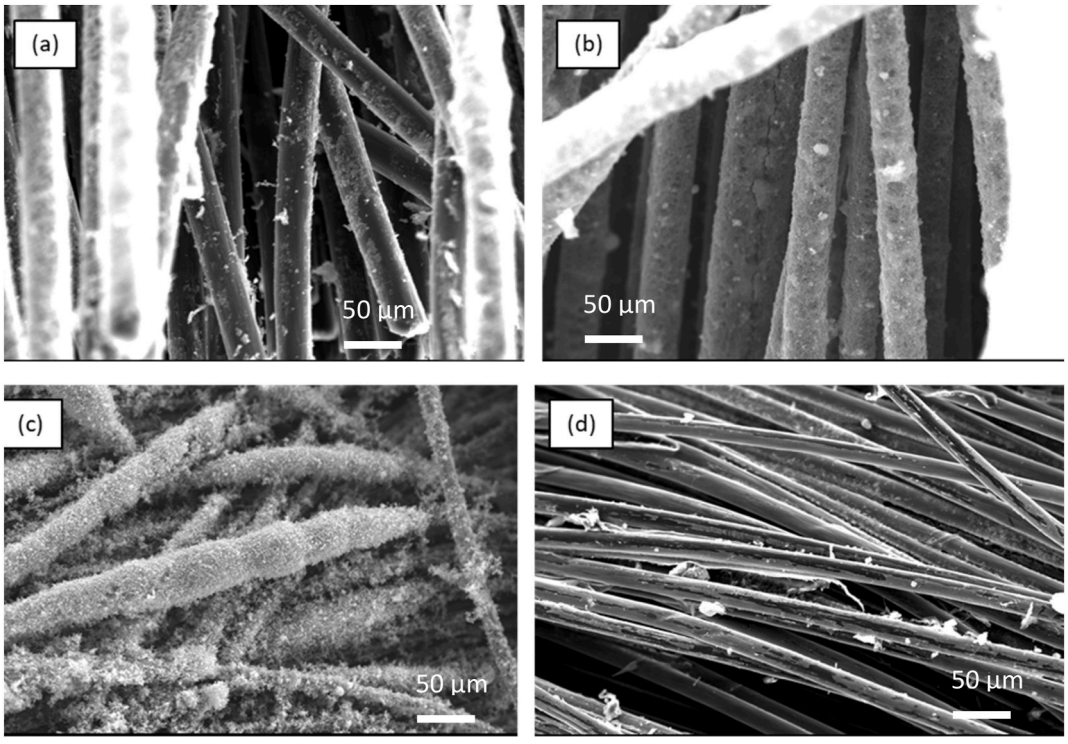

Fig. 5. SEM images of cathodes after (a) spraying 0.3 mg Pt cm^{-2}, (b) spraying 0.5 mg Pt cm^{-2}; (c) electrospraying 0.5 mg Pt cm^{-2} and (d) sputtering 0.01 mg Pt cm^{-2}.

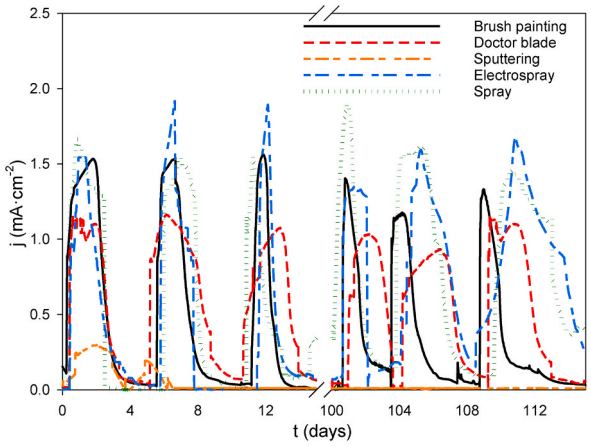

Fig. 6. Current density evolution of MECs with cathodes made using different Pt deposition techniques.

high H_2 production (1.98 m^3 $m^{-3}d^{-1}$), while doctor blade showed at maximum of 1.2 mA cm^{-2} and a production of H_2 of 1.55 m^3 $m^{-3}d^{-1}$, a 22 % lower than brush painting, electrospray, and spray techniques. This ranking of current densities correlated well with the Pt deposition observed in Fig. 3, where brush painting and doctor blade presented visually a lower active area, because the ink formed a compact layer with lower roughness, decreasing the electrode active area.

The cell with sputtering technique reported a current density of almost 0.3 mA cm^{-2}. Considering the Pt loading of this cathode (0.01 mg Pt cm^{-2}), 30.0 mA mg^{-1} Pt resulted to be a much higher specific current density compared with all other deposition techniques. However, the current density became almost null after mineral medium replacement. Pt detachment was observed multiple times upon contact with the medium even with the naked eye (*i.e.* the medium became dark) and confirmed by EDX measurements of the mineral medium (data not shown). Such poor stability of the sputtered cathode leads to discard this technique.

Fig. 7 shows the maximum current density along the cycles. All MECs (except that with the sputtered cathode) produced a stable maximum current density. The MEC with the electrosprayed cathode produced the highest current density until cycle 11. Thereafter, a slight decreased of the current density was observed. From cycle 11 onwards, the cell with the sprayed cathode showed the highest current density ($j_{max}^{average}$ = 1.68 ± 0.12 mA cm^{-2}) and displayed a more stable performance. However, the average current density was very similar for the sprayed cathode (1.68 mA cm^{-2}) and the electrosprayed cathode (1.67 mA cm^{-2}). Table 1 also shows that the H_2 production was not directly proportional to the current density. This means an uneven cathodic recovery which was attributed to H_2 leakages in the gas bag or H_2 recycling. The highest H_2 production was observed with the spray electrode with a Pt loading of 0.5 mg Pt cm^{-2}. In general, the amount of Pt per cm^2 was not directly proportional to the current density (neither considering the maximum current density nor the average current density). However, the cathodes modified by the electrospray and spray had a similar performance, which was proportional to the amount of Pt. At low Pt-loads, the electrode was not completely covered with Pt regardless of the technique used, there was not a continuity of Pt in the deposition on the surface. On the contrary, the Pt was distributed over the entire surface at Pt load of 0.5 mg Pt cm^{-2} (Fig. 5). The maximum specific current density (Table 1, mA mg^{-1} Pt) decreased by 17 % from 0.50 mg Pt cm^{-2} to 0.24 mg Pt cm^{-2} using electrospray, and by 33 % when decreasing the Pt loading to 0.15 mg Pt cm^{-2}. Using spray, the maximum specific current density is equal in the case of 0.5 mg Pt cm^{-2} and 0.13 mg Pt cm^{-2}, but it decreased by 12 % when changing the loading to 0.24 mg Pt cm^{-2}.

Fig. 8 shows the MEC performance parameters for the cells with different Pt deposition techniques. Most MEC provided CEs between 92 and 98 % (brush painting showed an unrealistic value of 102.6 %), which is a high value compared with other studies. For instance, using dewatered sludge the CE was almost 20 % lower than the cells used in this work [60] indicating that the consortium was well-adapted to acetate due its long-term operation or that a certain amount of H_2 was being recycled, *i.e.* part of the generated H_2 was scavenged by microorganisms. In addition, regarding the energy produced as H_2 compared to the energy input, Fig. 8 shows that the energy content in H_2 was only higher than that of the substrate but was lower than the electrical input. These values are usual in these lab-scale MECs. The values of r_{CAT} ranged between 75 and 95 %, indicating that a high amount of the current intensity was used for H_2 production and that the cell leakages were low.

A similar H_2 production of 1.98, 2.01 and 2.06 m^3 $m^{-3}d^{-1}$ was found for brush painting, electrospray and spray techniques, respectively, followed by doctor blade (1.55 m^3 $m^{-3}d^{-1}$) and sputtering (0.53 m^3

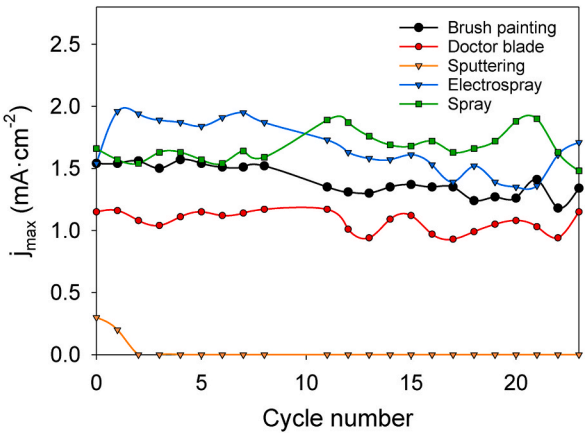

Fig. 7. Maximum current density at each cycle of MECs with cathodes made using different Pt deposition techniques.

Table 1
Characterization and performance of MECs with cathodes made using different Pt deposition techniques. Average data obtained from 23 cycles. Pt load was calculated by weighting. Experimental error is standard deviation (n = 23).

Deposition technique	Pt load (mg Pt cm^{-2})	j_{max} (mA cm^{-2})	j_{max} average (mA cm^{-2})	Maximum specific current density (mA mg^{-1} Pt)	Average maximum specific current density (mA mg^{-1} Pt)	H_2 production ($m^3m^{-3}d^{-1}$)
Brush painting	0.50	1.6	1.40 ± 0.12	3.2	2.8	1.98
doctor blade	0.50	1.2	1.07 ± 0.08	2.4	2.1	1.55
Electrospray	0.50	2.0	1.67 ± 0.21	4.0	3.3	2.01
	0.24	0.8	0.72 ± 0.03	3.3	3.0	1.09
	0.15	0.4	0.36 ± 0.02	2.7	2.4	0.82
Spray	0.50	1.9	1.68 ± 0.12	3.8	3.4	2.06
	0.24	0.8	0.75 ± 0.02	3.3	3.1	1.12
	0.13	0.5	0.39 ± 0.05	3.8	3.0	0.86
Sputtering	0.01	0.3	0.02 ± 0.07	30.0	2.0	0.53[a]

[a] Production during the first cycle of the cell only.

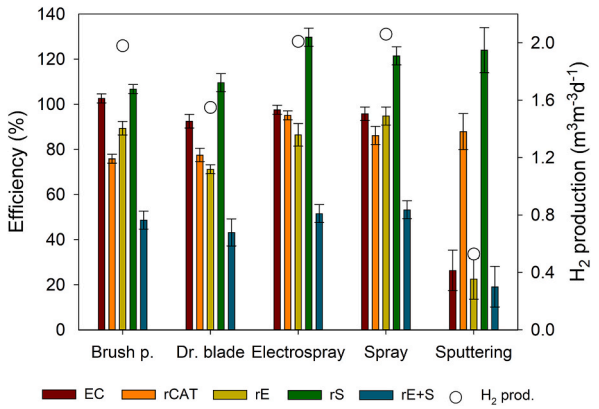

Fig. 8. The experimental value of CE, r_{CAT}, r_E, r_S, r_{E+S} and H_2 production on MECs for all cathodes coating with Pt. Error bars correspond to the standard deviation for n = 3 measurements.

$m^{-3}d^{-1}$) due to the fact that doctor blade cathode did not provide neither a homogeneous surface nor a high surface area, while sputtering led to Pt losses in contact with the medium. Furthermore, the H_2 concentration in all cells was above 77 % in each cycle, a high value, knowing that the remaining 23 % was mainly CO_2 and N_2. Finally, comparing the H_2 production values obtained with those of other published works, our production was much higher when compared with single-chamber cells with glycerol (between 1.3 and 0.6 m^3 $m^{-3}d^{-1}$) [61,63], cellulose (over 1.11 $m^3m^{-3}d^{-1}$) [62] or proteins (over 0.42 m^3 $m^{-3}d^{-1}$) [57].

The effect of the Pt deposition technique in the performance of MECs has been scarcely reported since brush painting stands out as the most employed [23]. Some authors studied the spraying technique to deposit Ni nanoparticles [28], Pt on carbon felt [64], while brush painting and spraying have also been used to deposit Pt on polymer electrolyte fuel cell cathodes [27]. Recently, 3D printing with a thing film coating has shown current densities of up to 46.63 mA cm^{-2} but with an applied a voltage of 1.7 V, making the energy expenditure significantly higher [65]. Kiely et al. [66] modified a cathode with brush painting with 0.5 mg Pt cm^{-2} in MECs to treat a dairy industry wastewater, achieving lower intensity, reaching 0.64 mA cm^{-2} in the best-case scenario. Conversely, research using wastewater from the dairy industry, a non-synthetic medium, demonstrated enhanced yields of H_2 production when employing cells with cathodes modified through the sputtering technique and electrospray [67,68]. The use of the spray technique to deposit Ni in MECs yielded almost one third of the current density (less than 0.5 mA cm^{-2}) than that obtained in this work with the electrospray technique. Overall, Pt is an optimal catalyst, but its deposition on the electrodes must be improved to make it viable on a large scale.

4. Conclusions

The use of spray and electrospray techniques for Pt deposition on carbon fibres resulted in a more accurate and homogeneous surface modification compared to bare carbon cloth, thereby enhancing performance. For cathodes with 0.5 mg Pt cm^{-2}, electrospray and spray techniques showed the best performance, with maximum current densities of 2.0 and 1.9 mA cm^{-2}, respectively. Average current densities were 1.67 ± 0.21 mA cm^{-2} for electrospray and 1.68 ± 0.12 mA cm^{-2} for spray, with H_2 yields of 2.01 and 2.06 m^3 $m^{-3}d^{-1}$. These techniques provided almost 20 % higher current density than brush-painted cathodes (1.40 mA cm^{-2}) and over 55 % higher than doctor blade cathodes (1.07 mA cm^{-2}). The better performance of spray and electrospray was attributed to selective Pt deposition on carbon fibres, confirmed by SEM and EDX analysis. The spray technique is labour-intensive and suitable for small-scale applications, whereas electrospray is automated and scalable. Regardless of the technique, the optimal Pt loading was 0.5 mg Pt cm^{-2}.

Spray and electrospray allowed a more customisable amount of Pt per cm^2 to be selected (tested values were 0.5, 0.24 and 0.15–0.13 mg Pt cm^{-2}), while maintaining a similar specific current density per mg of Pt added. Techniques such as doctor blade and brush painting produced compact layers that reduced the active surface area and cell performance. Sputtering was discarded due to Pt detachment.

With a Pt-loading of 0.5 mg Pt cm^{-2}, the CE was around 100 %, and, sometimes, exceeding it. In addition, H_2 production rates were similar to literature but lower than expected given the current density, suggesting H_2 leakage or H_2-recycling in cells. Rates of H_2 production were 2.06, 2.01, 1.98, and 1.55 m^3 $m^{-3}d^{-1}$ for spray, electrospray, brush painting, and doctor blade, respectively.

CRediT authorship contribution statement

Pilar Sánchez-Peña: Writing – original draft, Methodology, Investigation, Formal analysis, Data curation, Conceptualization. **Jesús Rodriguez:** Writing – review & editing, Methodology, Investigation, Formal analysis, Data curation. **Juan Antonio Baeza:** Writing – review & editing, Supervision, Formal analysis, Data curation, Conceptualization. **David Gabriel:** Writing – review & editing, Supervision, Formal analysis, Data curation, Conceptualization. **Albert Guisasola:** Writing – review & editing, Supervision, Project administration, Funding acquisition, Formal analysis, Data curation, Conceptualization. **Mireia Baeza:** Writing – review & editing, Supervision, Methodology, Formal analysis, Data curation.

Declaration of competing interest

The authors declare that they have no known competing financial interests or personal relationships that could have appeared to influence the work reported in this paper.

Acknowledgments

This work was supported by the grant CTQ2017-82404-R funded by MCIN/AEI/10.13039/501100011033 and by "ERDF A way of making Europe". Pilar Sánchez Peña is grateful to the FI predoctoral scholarship (2018FI_B01161) from the Catalan Government (Agència de Gestió d'Ajuts Universitaris i de Recerca). The authors are members of the GENOCOV research group (Grup de Recerca Consolidat de la Generalitat de Catalunya, 2021 SGR 515, www.genocov.com).

References

[1] Kadier A, Simayi Y, Abdeshahian P, Azman NF, Chandrasekhar K, Kalil MS. A comprehensive review of microbial electrolysis cells (MEC) reactor designs and configurations for sustainable hydrogen gas production. Alex Eng J 2016;55:427–43. https://doi.org/10.1016/j.aej.2015.10.008.

[2] Hansel A, Lindblad P. Towards optimization of cyanobacteria as biotechnologically relevant producers of molecular hydrogen, a clean and renewable energy source. Appl Microbiol Biotechnol 1998;50(50):153–60. https://doi.org/10.1007/S002530051270. 2 1998.

[3] Singh S, Jain S, Ps V, Tiwari AK, Nouni MR, Pandey JK, et al. Hydrogen: a sustainable fuel for future of the transport sector. Renew Sustain Energy Rev 2015;51:623–33. https://doi.org/10.1016/J.RSER.2015.06.040.

[4] Sewsynker Y, Kana EBG, Lateef A. Modelling of biohydrogen generation in microbial electrolysis cells (MECs) using a committee of artificial neural networks (ANNs). Biotechnol Biotechnol Equip 2015;29:1208–15. https://doi.org/10.1080/13102818.2015.1062732.

[5] Dincer I, Acar C. Review and evaluation of hydrogen production methods for better sustainability. Int J Hydrogen Energy 2014;40:11094–111. https://doi.org/10.1016/j.ijhydene.2014.12.035.

[6] Amores E, Rodríguez J, Oviedo J, Lucas-Consuegra A de. Development of an operation strategy for hydrogen production using solar PV energy based on fluid dynamic aspects. Open Eng 2017;7:141–52. https://doi.org/10.1515/ENG-2017-0020.

[7] Qadir M, Drechsel P, Cisneros BJ, Kim Y, Pramanik A, Mehta P, et al. Global and regional potential of wastewater as a water, nutrient and energy source. Nat Resour Forum 2020;44:40–51. https://doi.org/10.1111/1477-8947.12187.

[8] Islam AK. Hydropower coupled with hydrogen production from wastewater: integration of micro-hydropower plant (MHP) and microbial electrolysis cell (MEC). Int J Hydrogen Energy 2024;49:1–14. https://doi.org/10.1016/J.IJHYDENE.2023.06.179.
[9] Arun J, SundarRajan PS, Grace Pavithra K, Priyadharsini P, Shyam S, Goutham R, et al. New insights into microbial electrolysis cells (MEC) and microbial fuel cells (MFC) for simultaneous wastewater treatment and green fuel (hydrogen) generation. Fuel 2024;355:129530. https://doi.org/10.1016/J.FUEL.2023.129530.
[10] Logan BE, Call D, Cheng S, Hamelers HVM, Sleutels THJA, Jeremiasse AW, et al. Microbial electrolysis cells for high yield hydrogen gas production from organic matter. Environ Sci Technol 2008;42:8630–40. https://doi.org/10.1021/es801553z.
[11] Jiang J, Lopez-Ruiz JA, Bian Y, Sun D, Yan Y, Chen X, et al. Scale-up and techno-economic analysis of microbial electrolysis cells for hydrogen production from wastewater. Water Res 2023;241:120139. https://doi.org/10.1016/J.WATRES.2023.120139.
[12] Sharma A, Hussain Mehdi SE, Pandit S, Eun-Oh S, Natarajan V. Factors affecting hydrogen production in microbial electrolysis cell (MEC): a review. Int J Hydrogen Energy 2024;61:1473–84. https://doi.org/10.1016/J.IJHYDENE.2024.02.193.
[13] Wu X, Xie W, Ye J, Sun D, Ohnuki T, Li M, et al. Progress in heavy metals-containing wastewater treatment via microbial electrolysis cell: a review. J Water Proc Eng 2023;55:104228. https://doi.org/10.1016/J.JWPE.2023.104228.
[14] Lu L, Ren ZJ. Microbial electrolysis cells for waste biorefinery: a state of the art review. Bioresour Technol 2016;215:254–64. https://doi.org/10.1016/j.biortech.2016.03.034.
[15] Liu H, Grot S, Logan BE. Electrochemically assisted microbial production of hydrogen from acetate. Environ Sci Technol 2005;39:4317–20. https://doi.org/10.1021/es050244p.
[16] Srivastava P, García-Quismondo E, Palma J, González-Fernández C. Coupling dark fermentation and microbial electrolysis cells for higher hydrogen yield: technological competitiveness and challenges. Int J Hydrogen Energy 2024;52:223–39. https://doi.org/10.1016/J.IJHYDENE.2023.04.293.
[17] Gautam R, Ress NV, Wilckens RS, Ghosh UK. Hydrogen production in microbial electrolysis cell and reactor digestate valorization for biochar – a noble attempt towards circular economy. Int J Hydrogen Energy 2024;52:649–68. https://doi.org/10.1016/J.IJHYDENE.2023.07.190.
[18] Xu L, Li W, Luo J, Chen L, He K, Ma D, et al. Carbon-based materials as highly efficient catalysts for the hydrogen evolution reaction in microbial electrolysis cells: mechanisms, methods, and perspectives. Chem Eng J 2023;471:144670. https://doi.org/10.1016/J.CEJ.2023.144670.
[19] Jafary T, Yeneneh AM, Al-Hinai M. Role of microbial electrolysis desalination cell in sustainable water and energy management: performance assessment of platinum and nickel foam cathodes and simulating integration with reverse osmosis systems. Int J Hydrogen Energy 2024. https://doi.org/10.1016/J.IJHYDENE.2024.04.190.
[20] Lee HS, Torres CI, Parameswaran P, Rittmann BE. Fate of H2 in an upflow single-chamber microbial electrolysis cell using a metal-catalyst-free cathode. Environ Sci Technol 2009;43:7971–6. https://doi.org/10.1021/es900204j.
[21] Chae KJ, Choi MJ, Kim KY, Ajayi FF, Chang IS, Kim IS. A solar-powered microbial electrolysis cell with a platinum catalyst-free cathode to produce hydrogen. Environ Sci Technol 2009;43:9525–30. https://doi.org/10.1021/es9022317.
[22] Jeremiasse AW, Hamelers HVM, Buisman CJN. Microbial electrolysis cell with a microbial biocathode. Bioelectrochemistry 2010;78:39–43. https://doi.org/10.1016/j.bioelechem.2009.05.005.
[23] Middaugh J, Cheng S, Liu W, Wagner R. How to make cathodes with a diffusion layer for single-chamber microbial fuel cells. 2008.
[24] Li Qing, Yan Wenjun, Liu Ye, Du Haiyan, Zhongde Wang, Guan Guoqing. One-step electrodeposition of cauliflower-like CozNiySx@polypyrrole electrocatalysts on carbon fiber paper for hydrogen evolution reaction. Int J Hydrogen Energy 2019;44(26):12931–40. https://doi.org/10.1016/j.ijhydene.2019.03.218.
[25] Ivanov I, Ahn YT, Poirson T, Hickner MA, Logan BE. Comparison of cathode catalyst binders for the hydrogen evolution reaction in microbial electrolysis cells. Int J Hydrogen Energy 2017;42:15739–44. https://doi.org/10.1016/j.ijhydene.2017.05.089.
[26] Chaparro AM, Benítez R, Gubler L, Scherer GG, Daza L. Study of membrane electrode assemblies for PEMFC, with cathodes prepared by the electrospray method. J Power Sources 2007;169:77–84. https://doi.org/10.1016/J.JPOWSOUR.2007.01.044.
[27] Varga Á, Brunelli NA, Louie MW, Giapis KP, Haile SM. Composite nanostructured solid-acid fuel-cell electrodes via electrospray deposition. J Mater Chem 2010;20:6309–15. https://doi.org/10.1039/C0JM00216J.
[28] Manuel M-F, Neburchilov V, Wang H, Guiot SR, Tartakovsky B. Hydrogen production in a microbial electrolysis cell with nickel-based gas diffusion cathodes. J Power Sources 2010;195(17):5514–9. https://doi.org/10.1016/j.jpowsour.2010.03.061.
[29] Macak J, Pytel J, Ruiz JR, Beranek R. Photoelectrochemical properties of electrospun titania nanofibers - comparison with nanoparticles. MRS Online Proc Libr 2009;1211:74–80. https://doi.org/10.1557/PROC-1211-R08-34.
[30] Klaysom C, Ladewig BP, Lu GQM, Wang L. Preparation and characterization of sulfonated polyethersulfone for cation-exchange membranes. J Membr Sci 2011;368:48–53. https://doi.org/10.1016/J.MEMSCI.2010.11.006.
[31] Ali Ansari S, Mansoob Khan M, Omaish Ansari M, Hwan Cho M. Improved electrode performance in microbial fuel cells and the enhanced visible light-induced photoelectrochemical behaviour of PtOx@M-TiO2 nanocomposites. Ceram Int 2015;41:9131–9. https://doi.org/10.1016/J.CERAMINT.2015.03.321.
[32] González Rodríguez L, Campana Prada R, Sanchez-Molina M, Rodríguez Victoria TA. Study of the influence of Nafion/C composition on electrochemical performance of PEM single cells with ultra-low platinum load. Int J Hydrogen Energy 2020. https://doi.org/10.1016/j.ijhydene.2020.03.114.
[33] Sun L, Ran R, Wang G, Shao Z. Fabrication and performance test of a catalyst-coated membrane from direct spray deposition. Solid State Ionics 2008;179:960–5. https://doi.org/10.1016/J.SSI.2008.01.081.
[34] Muth J, Poggie M, Kulesha G, Meneghini RM. Novel highly porous metal technology in artificial hip and knee replacement: processing methodologies and clinical applications. JOM 2012;65(2):318–25. https://doi.org/10.1007/S11837-012-0528-5. 2012 65.
[35] Dobry DE, Settell DM, Baumann JM, Ray RJ, Graham LJ, Beyerinck RA. A model-based methodology for spray-drying process development. Journal of Pharmaceutical Innovation 2009;4(3):133–42. https://doi.org/10.1007/S12247-009-9064-4. 2009;4.
[36] Li W, Bi X, Luo M, Sui P-C. Numerical investigations on the ultrasonic atomization of catalyst inks for proton exchange membrane fuel cells. J Electrochem Soc 2021;168:034502. https://doi.org/10.1149/1945-7111/ABE725.
[37] Happe M, Sugnaux M, Cachelin CP, Stauffer M, Zufferey G, Kahoun T, Salamin PA, Egli T, Comninellis C, Grogg AF, Fischer F. Scale-up of phosphate remobilization from sewage sludge in a microbial fuel cell. Bioresour Technol 2016;200:435–43. https://doi.org/10.1016/J.BIORTECH.2015.10.057.
[38] Benítez R, Soler J, Daza L. Novel method for preparation of PEMFC electrodes by the electrospray technique. J Power Sources 2005;151:108–13. https://doi.org/10.1016/J.JPOWSOUR.2005.02.047.
[39] Ghasemi B, Yaghmaei S, Abdi K, Mardanpour MM, Haddadi SA. Introducing an affordable catalyst for biohydrogen production in microbial electrolysis cells. J Biosci Bioeng 2020;129:67–76. https://doi.org/10.1016/J.JBIOSC.2019.07.001.
[40] Martin S, Garcia-Ybarra PL, Castillo JL. Electrospray deposition of catalyst layers with ultra-low Pt loadings for PEM fuel cells cathodes. J Power Sources 2010;195:2443–9. https://doi.org/10.1016/j.jpowsour.2009.11.092.
[41] Benítez R, Soler J, Daza L. Novel method for preparation of PEMFC electrodes by the electrospray technique. J Power Sources 2005;151:108–13. https://doi.org/10.1016/J.JPOWSOUR.2005.02.047.
[42] Chingthamai N, Sombatmankhong K, Laoonual Y. Experimental investigation of electrospray coating technique for electrode fabrication in PEMFCs. Energy Proc 2017;105:1806–12. https://doi.org/10.1016/J.EGYPRO.2017.03.523.
[43] Sanchez J-L, Laberty-Robert C. A novel microbial fuel cell electrode design: prototyping a self-standing one-step bacteria-encapsulating bioanode with electrospinning. J Mater Chem B 2021;9:4309–18. https://doi.org/10.1039/D1TB00680K.
[44] Chae KJ, Kim KY, Choi MJ, Yang E, Kim IS, Ren X, et al. Sulfonated polyether ether ketone (SPEEK)-based composite proton exchange membrane reinforced with nanofibers for microbial electrolysis cells. Chem Eng J 2014;254:393–8. https://doi.org/10.1016/J.CEJ.2014.05.145.
[45] De las Heras A, Vivas FJ, Segura F, Andújar JM. From the cell to the stack. A chronological walk through the techniques to manufacture the PEFCs core. Renew Sustain Energy Rev 2018;96:29–45. https://doi.org/10.1016/J.RSER.2018.07.036.
[46] Çögenli MS, Mukerjee S, Yurtcan AB. Membrane electrode assembly with ultra low platinum loading for cathode electrode of PEM fuel cell by using sputter deposition. Fuel Cell 2015;15:288–97. https://doi.org/10.1002/FUCE.201400062.
[47] Lefebvre O, Tang Z, Fung MPH, Chua DHC, Chang IS, Ng HY. Electrical performance of low cost cathodes prepared by plasma sputtering deposition in microbial fuel cells. Biosens Bioelectron 2012;31:164–9. https://doi.org/10.1016/J.BIOS.2011.10.009.
[48] Fischer Fabian, Zufferey Géraldine, Sugnaux Marc, Happe Manuel. Microbial electrolysis cell accelerates phosphate remobilisation from iron phosphate contained in sewage sludge. Environ Sci Process Impacts 2014;17:90–7. https://doi.org/10.1039/C4EM00536H.
[49] Ul Z, Sánchez-Peña P, Baeza M, Sulonen M, Gabriel D, Baeza JA, et al. Systematic screening of carbon-based anode materials for bioelectrochemical systems. J Chem Technol Biotechnol 2023;98:1402–15. https://doi.org/10.1002/JCTB.7357.
[50] Sánchez-Peña P, Rodriguez J, Montes R, Baeza JA, Gabriel D, Baeza M, et al. Less is more: a comprehensive study on the effects of the number of gas diffusion layers on air–cathode microbial fuel cells. Chemelectrochem 2021;8:3416–26. https://doi.org/10.1002/CELC.202100908.
[51] Feng Y, Yang Q, Wang X, Logan BE. Treatment of carbon fiber brush anodes for improving power generation in air–cathode microbial fuel cells. J Power Sources 2010;195:1841–4. https://doi.org/10.1016/j.jpowsour.2009.10.030.
[52] Campana R, Sevilla G, Herradón C, Larrañaga A, Rodriguez J. Use of multi-injector for electrospinning of ceramic fibers in energy applications. Bol Soc Espanola Ceram Vidr 2019;58:238–45. https://doi.org/10.1016/j.bsecv.2019.01.003.
[53] Rojas N, Sánchez-Molina M, Sevilla G, Amores E, Almandoz E, Esparza J, et al. Coated stainless steels evaluation for bipolar plates in PEM water electrolysis conditions. Int J Hydrogen Energy 2021. https://doi.org/10.1016/J.IJHYDENE.2021.03.100.
[54] Kelly PJ, Arnell RD. Magnetron sputtering: a review of recent developments and applications. Vacuum 2000;56:159–72. https://doi.org/10.1016/S0042-207X(99)00189-X.
[55] Ribot-Llobet E, Montpart NN, Ruiz-Franco Y, Rago L, Lafuente J, Baeza JA, et al. Obtaining microbial communities with exoelectrogenic activity from anaerobic sludge using a simplified procedure. J Chem Technol Biotechnol 2014;89:1727–32. https://doi.org/10.1002/jctb.4252.
[56] Sánchez-Peña P, Rodriguez J, Gabriel D, Baeza JA, Guisasola A, Baeza M. Graphene functionalization with metallic Pt nanoparticles: a path to cost-efficient H2

production in microbial electrolysis cells. Int J Hydrogen Energy 2022;47:15397–409. https://doi.org/10.1016/J.IJHYDENE.2022.03.078.
[57] Montpart N, Rago L, Baeza JA, Guisasola A. Hydrogen production in single chamber microbial electrolysis cells with different complex substrates. Water Res 2015;68:601–15. https://doi.org/10.1016/j.watres.2014.10.026.
[58] Hyung-Sool Lee, Bruce E Rittmann. Significance of Biological Hydrogen Oxidation in a Continuous Single-Chamber Microbial Electrolysis Cell. Environ Sci Technol 2010;44(3):948–54. https://doi.org/10.1021/es9025358.
[59] Ambler JR, Logan BE. Evaluation of stainless steel cathodes and a bicarbonate buffer for hydrogen production in microbial electrolysis cells using a new method for measuring gas production. Int. J. Hydrogen Energy. 2011;36:160–6. https://doi.org/10.1016/j.ijhydene.2010.09.044.
[60] Hua T, Li S, Li F, Zhou Q, Ondon BS. Microbial electrolysis cell as an emerging versatile technology: a review on its potential application, advance and challenge. J Chem Technol Biotechnol 2019;94:1697–711. https://doi.org/10.1002/jctb.5898.
[61] Chignell JF, Liu H. Biohydrogen production from glycerol in microbial electrolysis cells and prospects for energy recovery from biodiesel wastes. ASME 2011 International Manufacturing Science and Engineering Conference, MSEC 2011 2011;1:693–701. https://doi.org/10.1115/MSEC2011-50274.
[62] Lalaurette E, Thammannagowda S, Mohagheghi A, Maness PC, Logan BE. Hydrogen production from cellulose in a two-stage process combining fermentation and electrohydrogenesis. Int J Hydrogen Energy 2009;34:6201–10. https://doi.org/10.1016/J.IJHYDENE.2009.05.112.
[63] Escapa A, Manuel MF, Morán A, Gómez X, Guiot SR, Tartakovsky B. Hydrogen production from glycerol in a membraneless microbial electrolysis cell. Energy Fuel 2009;23:4612–8. https://doi.org/10.1021/ef900357y.
[64] Rossi R, Nicolas J, Logan BE. Using nickel-molybdenum cathode catalysts for efficient hydrogen gas production in microbial electrolysis cells. J Power Sources 2023;560:232594. https://doi.org/10.1016/J.JPOWSOUR.2022.232594.
[65] Hüner B, Kıstı M, Özdoğan E, Demir N, Kaya MF. Pt thin film-coated 3D-printed polymer anode gas diffusion electrodes for PEM water electrolyzers. Energy & Fuels 2024. https://doi.org/10.1021/ACS.ENERGYFUELS.4C01342.
[66] Kiely PD, Cusick R, Call DF, Selembo PA, Regan JM, Logan BE. Anode microbial communities produced by changing from microbial fuel cell to microbial electrolysis cell operation using two different wastewaters. Bioresour Technol 2011;102:388–94. https://doi.org/10.1016/j.biortech.2010.05.019.
[67] Jayashree S, Ramesh ST, Lavanya A, Gandhimathi R, Nidheesh PV. Wastewater treatment by microbial fuel cell coupled with peroxicoagulation process. Clean Technol Environ Policy 2019;21:2033–45. https://doi.org/10.1007/S10098-019-01759-0.
[68] Ayuste C, Tinh VDC, Bose AB. Investigation of the catalyst ink compositions for a uniform microporous catalyst layer preparation via electrospray deposition technique and MEA assembling conditions in PEMFC specific. Solid State Ionics 2024;405:116452. https://doi.org/10.1016/J.SSI.2023.116452.